Tropical Aquatic and Soil Pollution

Research Article
Volume 6(1), 2026, 1–17
https://doi.org/10.53623/tasp.v6i1.1002

Optimisation of Photocatalytic Degradation for Enhancing Bathroom Greywater Quality Using 2,4,6-Trinitrotoluene/Zeolite Photocatalyst

Siti Nor Hidayah Arifin[1], Paran Gani[1]*, Radin Maya Saphira Radin Mohamed[2], Adel Al-Gheethi[3], Chin Wei Lai[4], G. Yashni[5], Kean Hua Ang[6]

[1]Department of Civil and Construction Engineering, Faculty of Engineering and Science, Curtin University Malaysia, Miri, 98009, Sarawak, Malaysia
[2]Micropollutants Research Centre (MPRC), Institute for Integrated Engineering (I2E), Universiti Tun Hussein Onn Malaysia (UTHM), 86400 Parit Raja, Batu Pahat, Johor, Malaysia
[3]Global Centre for Environmental Remediation (GCER), University of Newcastle, Newcastle, Australia
[4]Nanotechnology and Catalyst Research Centre (NanoCat), Universiti Malaya, 50603 Kuala Lumpur, Wilayah Persekutuan Kuala Lumpur, Malaysia
[5]Faculty of Engineering, Universiti Malaysia Sabah, Jalan UMS, 88400 Kota Kinabalu, Sabah, Malaysia
[6]Department of Geography, Faculty of Arts and Social Sciences, University of Malaya, Malaysia

*Correspondence: paran.gani@curtin.edu.my

SUBMITTED: 20 January 2026; REVISED: date; ACCEPTED: date

ABSTRACT: This experimental study investigated the solar photocatalytic degradation process for improving bathroom greywater quality using titanium dioxide nanotubes modified 2,4,6-trinitrotoluene with zeolite (TNTs/zeolite) and sought to optimize it. Organic pollutants, suspended solids, and personal care products remained in total household greywater at a proportion of 43–70% from bathroom sources. The optimization method applied was Central Composite Design (CCD) under Response Surface Methodology (RSM), in which three independent variables were considered: pH within a range of 3–10; catalyst loading expressed as the exposed surface area of 1 or 2 cm²; and irradiation time between thirty and one hundred eighty minutes under natural sunlight conditions with average irradiance values between six hundred twenty and seven hundred eighty watts per square meter. Twenty runs were carried out in triplicate. The responses tested were Biochemical Oxygen Demand (BOD), Chemical Oxygen Demand (COD), Total Suspended Solids (TSS), turbidity, pH, and Dissolved Oxygen (DO). The optimum condition predicted by RSM had a pH of 6.25, an irradiation time of 180 minutes, and a catalyst loading of 1 × 1 cm². Experimental validation at this optimum condition confirmed the adequacy of the model, with removals greater than 50% for COD, BOD, TSS, and turbidity. ANOVA showed that the models were statistically significant ($p < 0.0001$) and highly predictively reliable ($R^2 > 0.90$ for most responses). The study demonstrated that TNTs/zeolite under natural sunlight represented a potential low-energy alternative for bathroom greywater treatment with practical possibilities for decentralized reuse applications.

KEYWORDS: Optimisation; greywater quality; bathroom greywater; photocatalysis; TNTs/zeolite

1. Introduction

The quality of bathroom greywater needs to be considered carefully. Based on [1], light greywater is normally less contaminated and has lower concentrations of organic compounds and microorganisms than black greywater. Light greywater has been identified as a suitable candidate for water treatment systems for discharge purposes [2]. The chemical composition of greywater is typically classified into inorganic and organic constituents. Dissolved matter, non-metallic components, nutrients, metals, and gases are included in the inorganic constituents. Meanwhile, organic constituents are represented by several parameters such as BOD, COD, turbidity, pH, and TSS [3, 4]. The production of greywater from residential areas has increased dramatically with population growth [4]. It is estimated that about 6 million tonnes of domestic wastewater are produced every year in Malaysia. This huge amount of domestic wastewater can significantly impact quality of life if it is freely discharged into waterways such as surface waters. In fact, in some rural areas of Malaysia, domestic wastewater is directly discharged into rivers. Therefore, this situation needs to be handled and mitigated wisely, since domestic wastewater is considered a complex mixture containing water and common constituents such as organic compounds influenced by personal care products [5, 6]. Greywater from ablution, sinks, laundry, and bathrooms contains concentrations of organic and inorganic compounds influenced by pharmaceutical and personal care products (PPCPs), which may have negative effects on human health [7] and the environment [6]. Addressing these problems requires extensive research to identify effective water purification methods that can be considered green technologies, with lower energy consumption and minimal chemical usage while reducing environmental impacts [8].

Conventional greywater treatment methods such as adsorption, filtration, and flocculation have been proven to be insufficient and may generate secondary pollution [9]. Greywater quality enhancement via photocatalytic degradation under natural sunlight appears to be an alternative method due to the presence of various organic pollutants in greywater, especially bathroom greywater. Photocatalytic degradation is a promising advanced oxidation process (AOP) for the degradation of pollutants in aqueous solutions, with efficiency depending on catalyst concentration, leading to structural decomposition and a decrease in total organic carbon (TOC) [10–12]. TiO_2 is one of the most promising photocatalysts and has received special attention due to its wide band gap and the absence of toxic intermediate by-products, as H_2O and CO_2 are the final products [8, 13]. However, TiO_2 alone is inadequate to maintain prolonged and stable photocatalytic performance. Therefore, this study presents a modified catalyst called TNTs/zeolite, in which TiO_2 nanotubes are coated with zeolite powder. In heterogeneous photocatalysis, the main reaction is activated on the photocatalyst surface by a specific wavelength of light, involving either sunlight or UV radiation [14]. This process is highly effective in treating wastewater due to the strong oxidation by hydroxyl radicals generated under light irradiation, which can attack the chemical bonding structures of xenobiotic organic compounds (XOCs) present in water [14–18]. Many studies have investigated photocatalytic degradation using artificial UV light, and it has been proven to be very effective in degrading pollutants in water. It has been reported that photocatalytic degradation efficiencies using sunlight and UV light were 50% and 33%, respectively [19, 20]. However, photocatalytic degradation using sunlight requires further environmental optimization to enhance photocatalytic activity [14, 18]. The efficiency of photocatalytic

degradation of XOCs depends on the initial reactant concentration, solar UV radiation, catalyst type and loading, pH, temperature, irradiation time, and oxygen concentration [8. 19, 20].

The pH value plays an important role in the photocatalytic degradation rate of organic compounds, as characteristics such as particle size and surface charge of photocatalysts are closely related to pH due to the amphoteric behavior of most photocatalyst oxides [21, 22]. Moreover, the TiO_2 photocatalyst reaches its zero-point charge (ZPC) at pH 6.2. In acidic solutions with pH values below 6.2, the TiO_2 surface becomes positively charged, whereas under alkaline conditions with pH values above 6.2, the surface becomes negatively charged [22]. In addition, prolonged irradiation time not only enables more compound molecules to be photocatalyzed by TiO_2 but also activates the photocatalyst to generate more hydroxyl and superoxide radicals, leading to increased photodegradation of compounds. Catalyst loading also plays a significant role in achieving efficient photocatalytic degradation. Many studies have reported TiO_2-based photocatalysis of greywater under artificial UV light. However, statistical optimization studies of TNTs/zeolite performance under natural sunlight are very limited, creating the novelty of this work. To the best of our knowledge, no previous study has applied RSM with CCD to optimize the photocatalytic degradation of artificial bathroom greywater (ABGW) using TNTs/zeolite under solar irradiation. Therefore, this experimental work aims to statistically optimize and validate a predictive model for the photocatalytic degradation of ABGW using TNTs/zeolite under natural sunlight, where the effects of pH, irradiation time, and catalyst loading are investigated using RSM-CCD.

2. Materials and Methods

2.1. Greywater sample collection.

Greywater from bathing, showering, and hand-washing sinks was used in this study, and sampling was conducted at Parit Haji Salleh (1° 54’ 0” N, 103° 9’ 0” E), located in Parit Raja, Batu Pahat, Johor. Samples were collected from the discharge points of four houses. Grab samples were obtained for three consecutive days to determine the effluent disposal characteristics and discharge patterns. Sampling was conducted three times per day between 6–8 am, 12–2 pm, and 7–9 pm using the grab sampling method according to standard procedures to ensure that variations in effluent content were captured. Samples were stored in polyethylene terephthalate (PET) plastic bottles. The samples were then transported and analyzed according to standard methods in the university environmental laboratory within 24 hours to determine the initial characteristics of the effluent.

2.2. ABGW preparation.

ABGW was formulated by Anwar et al. [23] to contain constituents typically found in actual greywater, including nutrients, as shown in Table 1. To evaluate and compare the performance of several treatment processes, experiments were conducted using ABGW to ensure that the effluent was reproducible and representative of household greywater. ABGW was reconstituted so that its physicochemical and microbiological parameters were consistent with those of real greywater. Some authors have used mixtures of chemical substances and commercial hygiene products to simulate greywater composition [24]. However, these products may vary in composition over time and may not be universally available; therefore, to ensure reproducibility, ABGW was composed exclusively of technical-grade chemical products [25].

Table 1. ABGW recipe.

PPCPs	Amount (mg/l)	Product Brand
Shampoo	1	Sunsilk
Showergel	0.55	Lifebuoy
Toothpaste	0.64	Colgate
Soap	1	Palmolive
Detergent	0.63	K1000

2.3. Synthesis of photocatalyst.

The substrate sample (Ti foil, dimensions 5 cm × 1 cm) was ultrasonically cleaned in acetone for 10 minutes, then rinsed with deionized water and dried in air. The titanium substrate was subsequently anodized in a two-electrode electrochemical setup using a platinum rod; the Ti foil served as the anode, while the platinum rod acted as the cathode [26]. The electrolyte solution containing fluoride ions used in the electrochemical anodization process was an ethylene glycol-based electrolyte (ethylene glycol 98%, v/v; H_2O 2%, v/v; NH_4F 0.09 M). Each substrate sample was anodized for 1 hour at an applied voltage ranging from 10 V to 60 V using a DC power supply. The actual current and potential of the Ti electrode were measured and recorded manually. After anodization, the obtained samples were rinsed with acetone and deionized water, dried in air at 80°C for 24 hours, and then calcined at 450°C (heating rate 2°C/min) for 1 to 6 hours [27]. Pure TiO_2 nanotubes were modified with zeolite as transition metal-based particles to produce TNTs/zeolite by direct surface adsorption of metal ions or metal precursor particles (zeolite) from alcoholic solutions or suspensions, followed by electrophoretic deposition [26, 28]. The type of modifier was indicated on the sample label. To prepare the modified nanotubes, a specified amount of precursor solution was applied onto the surface of the pure nanotubes using an applied voltage of 60 V for 30 seconds during electrophoretic deposition. Zeolite powder (2 g/l) was added to the alcoholic solution and sonicated to ensure uniform dispersion. After zeolite deposition, the samples were dried at 80°C for 24 hours in a drying oven and then calcined at 450°C for 3 hours.

2.4. Photocatalytic experiment.

Photocatalytic experiments were performed outdoors from 11:00 to 16:00 under natural sunlight. A calibrated solar power meter registered an average irradiance between 620 and 780 W/m² during the experiment. Weather conditions were recorded, and all experiments were conducted on clear-sky days within a single day to reduce variability. All experiments were run in triplicate, and the mean values and standard deviations were reported. Outliers were tested using Grubbs' test at a 95% confidence level. No statistically significant outliers were detected. The optimum condition determined by RSM was validated through confirmation experiments carried out under the predicted optimum parameters. The experimental results differed by less than 5% from the predicted values, confirming the adequacy of the model.

2.5. Parameter (pollutant) reduction analysis.

An oxidation method was used to measure pollutant concentrations before and after each experimental run. The percentage of pollutant reduction was calculated using the following equation:

$$Pollutant\ Reduction\ (\%) = \frac{A^0 - A}{A_0} x\ 100$$

where A^0 is the value before treatment and A is the value after the treatment process. Each experiment was performed in triplicate.

2.6. Design experiment, statistical analysis and optimization.

A three-variable, three-level Response Surface Methodology–Face Centered Central Composite Design (RSM-FCCD) was employed with 20 experimental runs. The variables and their selected levels for the photocatalytic degradation of ABGW were reaction time (30–180 min), pH (3–10), and catalyst foil size (1–2 cm²), as shown in Table 2. Water quality parameters such as BOD, COD, TSS, pH, and turbidity were analyzed as responses. The FCCD design matrix is presented in Table 2. For statistical analysis, the variables were coded according to the following equation:

$$\alpha = \frac{x_i - x_0}{\Delta x}$$

w where α is the coded value of the independent variable, x_i is its real value, x_0 is its real value at the center point, and Δx is the step change in the variable x_i.

Table 2. Composition of various experiments of FCCD.

Exp No.	Factors			Removal					
	pH	Time (min)	Catalyst Size (cm)	TSS (%)	COD (%)	BOD (%)	Turbidity (%)	pH	DO (mg/l)
1	6.5	180	1.5	41.9303	56.14731	64.5718	51.32967	7.0933	9.510
2	3	180	1	79.6622	57.6204	97.7434	83.69544	3.28	10.120
3	10	180	1	14.0997	26.5722	42.0061	32.83495	7.4067	10.417
4	10	105	1.5	13.8321	23.1728	40.9681	19.20726	7.85	9.313
5	3	30	2	72.7046	60.1133	63.8046	74.69143	3.87	10.333
6	6.5	105	1.5	30.9586	43.87158	50.4457	49.62621	7.09	8.760
7	6.5	105	1.5	50.7612	51.5581	49.1369	63.74061	7.06	8.700
8	3	180	2	78.0566	68.27195	94.2232	82.47868	4.1167	8.990
9	10	180	2	30.6910	22.9084	41.5096	41.1089	8.0267	8.920
10	6.5	105	1.5	48.0852	57.67705	50.2200	60.09033	7.23	8.713
11	6.5	105	1.5	37.3811	57.84703	46.0228	55.95335	7.15	8.733
12	10	30	1	2.8604	9.102927	6.21686	21.88413	7.9067	11.133
13	3	30	1	81.5355	57.4693	52.1155	83.93879	4.7567	10.810
14	6.5	105	1.5	47.2824	55.1841	57.3149	46.709	4.1367	9.330
15	3	105	1.5	68.9581	57.6015	65.339	71.5279	7.2467	9.263
16	6.5	105	1.5	39.5219	54.1643	52.2058	53.03313	7.28	8.817
17	6.5	105	1	43.0007	51.5203	43.2698	35.7552	7.3367	9.600
18	6.5	30	1.5	30.4234	50.31161	48.6855	55.95335	7.15	8.710
19	6.5	105	2	35.7755	54.80642	58.2985	43.05572	7.33	9.230
20	10	30	2	13.0293	28.44193	18.3572	38.1887	8.04	11.167

Design-Expert software (Version 11) was employed in this study. After evaluating increasingly complex models, ranging from linear to partial cubic, a partial cubic polynomial model was selected to investigate the effects of the variables on pollutant degradation. The final equation of the developed model is presented as follows:

$$y = \beta^0 + \beta^1 x^1 + \beta^2 x^2 + \beta^3 x^3 + \beta^{12} x^1 x^2 + \beta^{13} x^1 x^3 + \beta^{23} x^2 x^3 + \beta^{11} x^{21}$$

$$+\beta_{22}x^2{}_2 + \beta_{33}x^2{}_3 + \beta_{112}x^2{}_1x_2 + \beta_{113}x^2{}_1x_3$$

where y represents the response variable (degradation efficiency). β_0 is the intercept; β_i are the regression coefficients for linear effects; β_{ij} are the regression coefficients for interaction effects; β_{ii} are the regression coefficients for quadratic effects; β_{iij} are the regression coefficients for cubic effects; and x_i represents the coded experimental levels of the variables.

The percentage of pollutant reduction could be related to the independent variables by a quadratic model expressed as:

$$y = \beta^0 + \sum_{i=1}^{k} \beta_i x_i + \sum_{i=1}^{k} \beta_{ii} x^2{}_i + \left(\sum^{k-1} \quad \sum^{k} \beta_{il} x_i x_l\right.$$

where y is the response; x_i and x_l are the independent variables; β_0 is the constant coefficient; and β_i, β_{ii}, and β_{il} are the coefficients for linear, quadratic, and interaction (second-order) terms, respectively.

Analysis of variance (ANOVA) was used to determine whether the generated models adequately described the experimental data. Optimization was performed using a desirability function in the software. The experiment with a desirability value of 1 was selected as the optimum condition, calculated using the following equation:

$$D = \left(d^1 \quad x \quad d^2 \quad x \ldots \quad x \, d_n\right)^{\frac{1}{n}} = \left(\prod^{n} d_i\right)^{\frac{1}{n}}$$

where n is the number of responses considered and d_i represents the desirability value for each response.

3. Results and Discussion

3.1. Bathroom greywater quality.

The ABGW recipe was adopted from Anwar et al. [23], as presented in Table 1. The quality of ABGW was determined based on several parameters, including pH, TSS, turbidity, COD, and BOD. These selected parameters were analyzed, and the results were used as reference points to evaluate the pollution strength. The main indicators considered were BOD, COD, pH, and turbidity. The characteristics of raw bathroom greywater obtained from the houses involved in the case study are presented in Table 3. For ABGW, the COD value was 447 mg/l, while the BOD value was 156 mg/l. In comparison, the raw bathroom greywater showed a COD value of 533 mg/l and a BOD value of 148 mg/l. Mohamed et al. [29] reported COD values ranging from 445 to 621 mg/l and BOD values between 40 and 105 mg/l. Hourlier et al. [25] and Eriksson et al. [6] recorded COD values of 454 mg/l and 100–633 mg/l, respectively, while the corresponding BOD values were approximately 129 mg/l and 170 mg/l. The variability among samples reflects differences in lifestyle, customs, sanitary installations, product preferences, and washing habits of the population.

Table 3. Comparison of artificial and raw bathroom greywater characteristics with previous studies (n = 5).

Parameter	ABGW			Raw Bathroom Greywater		
	This Study	Mohamed et al. [1]	Hourlier et al. [25]	This Study	Mohamed et al. [29]	Eriksson et al. [6]
pH	6.61 ± 0.89	n.a.	6.76	6.3	6.1–6.5	6.7–7.4
Turbidity (NTU)	62 ± 1.64	n.a.	24	65.7	n.a.	49–92
BOD_5 (mg/l)	156 ± 7.21	n.a.	65	148	40–105	170
COD (mg/l)	447 ± 8.37	157	454	533	445–621	100–633

3.3. RSM.

3.3.1. COD removal.

As COD indicates the extent of degradation of organic species, the percentage change in COD was investigated in this study. COD reduction represents the degree of mineralization at the end of the photocatalytic process [30]. The experimental data, together with the obtained percentage reduction of COD, are presented in Table 4. According to ANOVA, a quadratic polynomial model was statistically significant in representing the relationship between the response (COD reduction) and the variables, as indicated by a small p-value (< 0.0001), an insignificant lack of fit, and a high coefficient of determination ($R^2 = 0.9440$). The ANOVA results for the model are shown in Table 4. The model equation in terms of coded factors is given below:

$$COD\ reduction = 53.19 - 19.09A + 2.61B + 3.23C + 0.4523AB + 0.2975AC - 1.87BC - 12.52A^2 + 0.3185B^2 + 0.2524C^2$$

where A represents pH, B represents irradiation time, and C represents catalyst loading.

Among the variables studied, pH was found to have the greatest effect on COD reduction, with the highest F-value of 133.83. The effects of pH and catalyst loading on the response were statistically significant. Figure 1(a) illustrates the three-dimensional response surface showing the combined effect of pH and catalyst loading on COD reduction. As the pH of the solution decreased, COD reduction increased, and the maximum response was observed at pH 3 with a catalyst loading of 2 × 1 cm^2. This behavior may be attributed to the formation of reactive oxygen species at lower pH, which can effectively attack the chemical bonds of COD-related pollutants during the photocatalytic reaction, leading to bond cleavage and degradation of functional groups. At higher pH, hydroxyl radicals further decompose intermediate molecules into smaller fragments, resulting in a gradual decrease in COD over time [31]. Maximum COD reduction was achieved at the highest catalyst loading. This is because an increased catalyst loading enhances the available active surface area of TNTs/zeolite, thereby increasing the photodecomposition rate. Adequate catalyst loading promotes the photogeneration of electron–hole pairs, which enhances the overall COD reduction efficiency [32].

Table 4. ANOVA for COD reduction.

Source	Sum of Squares	df	Mean Square	F-value	p-value	
Model	4588.62	9	509.85	18.73	< 0.0001	significant
A-pH	3643.45	1	3643.45	133.83	< 0.0001	

B-Time	68.02	1	68.02	2.50	0.1450	
C-TNTs Size	104.05	1	104.05	3.82	0.0791	
AB	1.64	1	1.64	0.0604	0.8109	
AC	0.7078	1	0.7078	0.0260	0.8751	
BC	28.11	1	28.11	1.03	0.3335	
A^2	431.33	1	431.33	15.84	0.0026	
B^2	0.2789	1	0.2789	0.0102	0.9214	
C^2	0.1752	1	0.1752	0.0064	0.9376	
Residual	272.24	10	27.22			
Lack of Fit	136.22	5	27.24	1.00	0.4994	not significant
Pure Error	136.02	5	27.20			
Cor Total	4860.86	19				

The effect of varying pH and contact time on COD reduction is shown in Figure 1(b). The maximum COD reduction was observed at pH 6.5 and an irradiation time of 180 minutes. However, longer irradiation times were required to achieve this maximum reduction [33]. Figure 1(c) illustrates the effect of varying irradiation time and catalyst size on COD reduction. According to ANOVA, the interaction effect between time and catalyst loading was not statistically significant; however, to maintain an insignificant lack of fit, the BC interaction term was retained in the model. The maximum COD reduction was observed at 180 minutes using a catalyst size of 2 × 1 cm (TNTs/zeolite). The enhanced reduction is attributed to the longer contact time and the increased availability of active sites on the catalyst surface, which together promote higher COD removal efficiency.

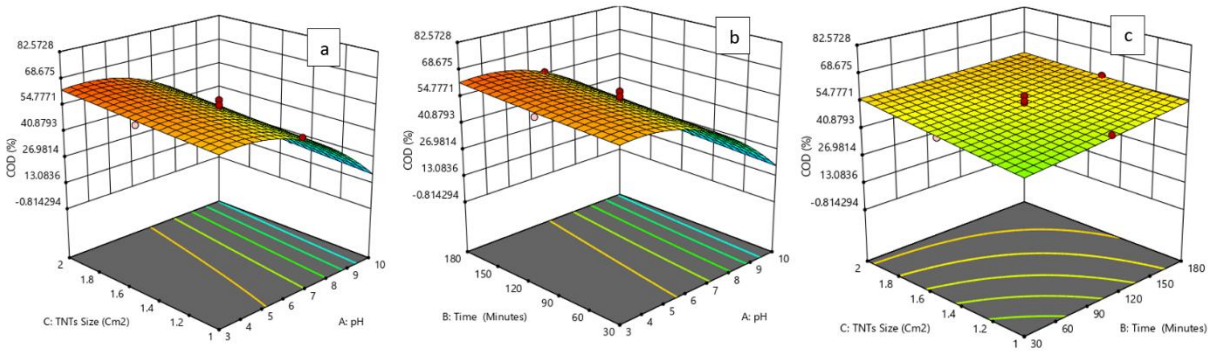

Figure 1. 3-D response surface of COD reduction using photocatalytic degradation, a) pH and catalyst, b) pH and contact time c) catalyst and time.

3.3.2. BOD removal.

The design matrix of the variables, along with the obtained BOD reduction percentages, is presented in Table 2. Fitting the experimental data to various models and subsequent ANOVA indicated that the photocatalytic process was most appropriately described by a partial cubic model. The model equation in terms of coded factors is as follows:

$$BOD\ reduction = 52.12 - 22.42A + 15.09B + 3.48C$$

where A represents pH, B represents irradiation time, and C represents catalyst loading.

The ANOVA results for the model are shown in Table 5. The lack of fit, which measures the variation of data around the fitted model, was evaluated using an F-test. The model showed

no significant lack of fit, indicating its adequacy. The F-value of the model (57.23) with a p-value less than 0.0001 implies that the model is statistically significant at the 95% confidence level. The high coefficient of determination ($R^2 = 0.9148$) further supports the suitability of the model in representing the actual relationship among the variables [31]. The predicted R^2, which indicates the model's predictive ability for new observations, was 0.9000, in reasonable agreement with the adjusted R^2 of 0.9148. Adequate precision, which measures the signal-to-noise (S/N) ratio, was 27.879 for this model—well above the minimum acceptable value of 4—indicating that the model can reliably navigate the design space. The significance of each term in the model was evaluated by testing the null hypothesis. In this case, A (pH) and B (irradiation time) were significant model terms, while C (catalyst loading) was not. The developed model was subsequently used to study the effects of operational parameters on the BOD reduction efficiency of TiO_2 nanotubes.

Table 5. ANOVA for BOD reduction.

Source	Sum of Squares	df	Mean Square	F-value	p-value	
Model	7422.83	3	2474.28	57.23	< 0.0001	significant
A-pH	5025.12	1	5025.12	116.24	< 0.0001	
B-Time	2276.31	1	2276.31	52.65	< 0.0001	
C-TNTs Size	121.39	1	121.39	2.81	0.1132	
Residual	691.71	16	43.23			
Lack of Fit	621.29	11	56.48	4.01	0.0685	not significant
Pure Error	70.42	5	14.08			
Cor Total	8114.54	19				

Figures 2(a) and 2(b) depict the three-dimensional (3D) response surface plots showing the effect of catalyst loading, pH, and their interactions on BOD reduction at 15.5 minutes (the center point of the experimental design). At pH 3, increasing the catalyst dose did not significantly affect BOD reduction, and even a low amount of catalyst resulted in a high BOD reduction percentage. Minimum BOD removal was observed at high pH combined with low catalyst loading. Catalyst loading (TiO_2) in the photocatalytic water treatment system directly influences the reaction rate [34]. Increasing the catalyst loading enhances the number of active sites on the catalyst surface, which increases the generation rate of electron–hole pairs and, consequently, BOD reduction [35]. However, beyond a certain catalyst loading, the available pollutant molecules become insufficient for adsorption on the increased TNTs/zeolite surface. As a result, additional catalyst particles do not contribute to the reaction, and the reaction rate tends to plateau [36]. Determining the optimum catalyst loading is therefore critical for efficient pollutant removal. Excess photocatalyst can increase solution turbidity, reducing UV light penetration [35], and higher catalyst loadings above the saturation level can lead to particle aggregation and reduced irradiation efficiency due to light scattering by TNTs/zeolite and increased opacity [34].

According to ANOVA, pH had the greatest effect on BOD reduction, with the highest F-value of 116.24. In heterogeneous photocatalysis, solution pH influences the surface charge of catalyst particles, the positions of the conduction and valence bands, and the ionization state of BOD molecules [36]. However, interpreting the effect of pH is complex because multiple mechanisms are involved, including hydroxyl radical attack, direct oxidation by positive holes,

and direct reduction by electrons in the conduction band [37]. Figure 2(c) shows the effect of varying pH and irradiation time on BOD reduction. Prolonging the irradiation time significantly enhanced BOD reduction at pH values below 4.0. The highest BOD reduction (97.7%) was observed at pH 3 with 180 minutes of irradiation. At pH 6.5, maximum BOD reduction was also achieved at 180 minutes. At this pH, the effect of irradiation time was highly significant, with an increase from 30 to 180 minutes resulting in a 64.6% increase in BOD reduction.

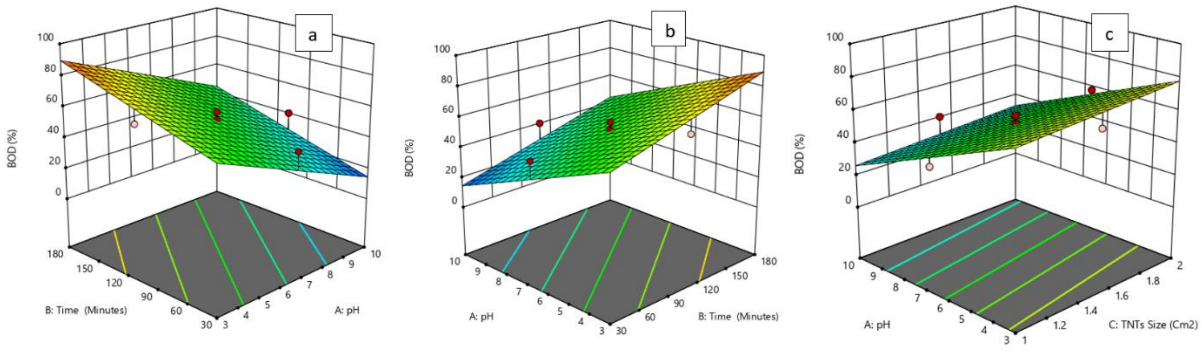

Figure 2. 3-D response surface of BOD reduction using photocatalytic degradation, a) time and pH, b) pH and time, c) pH and catalyst.

3.3.3. TSS Removal.

The ANOVA results for TSS reduction via photocatalytic degradation, based on experiments designed using RSM, are summarized in Table 6. The model p-value was <0.0001, indicating that the model is statistically significant. The lack-of-fit value of 0.9173 suggests that the lack of fit is not significant relative to the pure error, with a 58.2% probability that the lack-of-fit F-value could occur due to random noise. This nonsignificant lack of fit confirms the model's good predictability. The predicted R^2 of 0.8548 is in reasonable agreement with the adjusted R^2 of 0.9005, further supporting the model's predictive capability. The relationship between the independent variables and TSS reduction is described by the following equation:

$$TSS = 43.03 - 30.64A + 4.39B - 0.9098C$$

where A represents pH, B represents irradiation time, and C represents catalyst loading.

Table 6. ANOVA for TSS reduction

Source	Sum of Squares	df	Mean Square	F-value	p-value	
Model	9589.26	3	3196.42	58.35	< 0.0001	significant
A-pH	9388.37	1	9388.37	171.37	< 0.0001	
B-Time	192.60	1	192.60	3.52	0.0792	
C-TNTs Size	8.28	1	8.28	0.1511	0.7026	
Residual	876.53	16	54.78			
Lack of Fit	586.11	11	53.28	0.9173	0.5820	not significant
Pure Error	290.42	5	58.08			
Cor Total	10465.78	19				

Three-dimensional (3D) surface plots provide a graphical representation of the regression equation for optimizing reaction conditions and are particularly useful for visualizing the

behavior of the reaction system. The interactions between the three independent variables and the dependent variable (TSS reduction) are shown in Figure 3. Figures 3(a) and 3(b) illustrate the interaction effect of pH and irradiation time on the TSS reduction rate. The response surfaces indicate an inclined, nearly flat profile, showing that as pH and irradiation time approach their optimum values, the TSS reduction rate approaches its maximum. Figure 3(c) shows the interaction effect of pH and catalyst loading on TSS reduction. The surface similarly exhibits an inclined flat profile. TSS reduction increased with increasing pH, regardless of whether the catalyst loading was at a low or high level. Specifically, an increase in TSS reduction was observed as pH increased from 3 to 6 and catalyst loading increased from 1 cm² to 2 cm². Beyond these optimum values, further increases in pH or catalyst loading did not enhance TSS reduction, indicating that the interaction effect plateaus once the optimum conditions are reached.

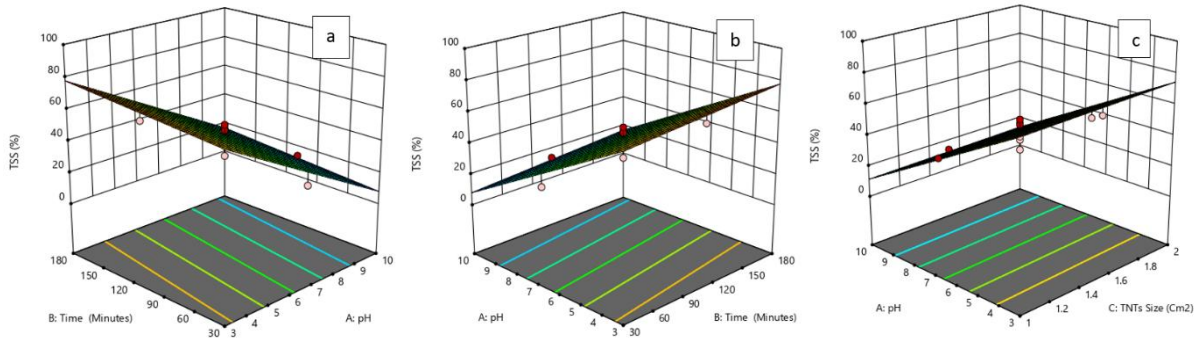

Figure 3. 3-D response surface of TSS reduction using photocatalytic degradation, a) time and pH, b) pH and time, c) pH and catalyst.

3.3.4. pH neutralization.

The ANOVA results for pH neutralization are summarized in Table 7. High correlation coefficients ($R^2 = 0.9948$ and adjusted $R^2 = 0.9900$) indicate a close fit between the predicted and experimental values. The model F-value of 210.97, along with very low p-values (<0.0001), demonstrates that the model is statistically significant, and all model terms are significant. The lack-of-fit test was not significant, confirming the adequacy of the model. As shown in Table 7, the F-values for the main effects of pH (A), irradiation time (B), and catalyst loading (C) were 1516.60, 13.51, and 0.7711, respectively, indicating that pH is the most significant factor, followed by irradiation time and catalyst loading. Among the interaction terms, BC had the highest F-value (31.68), followed by AB (2.68) and AC (1.50), indicating that the interaction between irradiation time and catalyst loading (BC) was the most significant for pH neutralization. The model equation in terms of coded factors is given as:

$$\text{pH neutralization} = 7.20 + 1.91A - 0.18B + 0.043C + 0.0896AB + 0.0671AC + 0.3096BC - 1.24A^2 - 0.116B^2 + 0.0952C^2$$

where A represents pH, B represents irradiation time, and C represents catalyst loading.

Table 7. ANOVA for pH neutralization.

Source	Sum of Squares	df	Mean Square	F-value	p-value

Model	45.53	9	5.06	210.97	< 0.0001	significant
A-pH	36.37	1	36.37	1516.60	< 0.0001	
B-Time	0.3240	1	0.3240	13.51	0.0043	
C-TNTs Size	0.0185	1	0.0185	0.7711	0.4005	
AB	0.0642	1	0.0642	2.68	0.1328	
AC	0.0360	1	0.0360	1.50	0.2485	
BC	0.7667	1	0.7667	31.98	0.0002	
A^2	4.26	1	4.26	177.72	< 0.0001	
B^2	0.0373	1	0.0373	1.56	0.2405	
C^2	0.0249	1	0.0249	1.04	0.3322	
Residual	0.2398	10	0.0240			
Lack of Fit	0.1995	5	0.0399	4.96	0.0518	not significant
Pure Error	0.0403	5	0.0081			
Cor Total	45.77	19				

The three-dimensional (3D) surface plot of pH photo-neutralization as a function of pH and irradiation time is shown in Figure 4(a). The shape of the plot indicates that the interaction between pH and irradiation time has a modest effect on pH photo-neutralization. As observed, when pH is below 6.5, increasing irradiation time enhances pH neutralization. In previous studies, RSM was used to optimize the photocatalytic performance of TiO_2 nanotubes under simulated sunlight [38]. Those authors reported that irradiation time had the greatest impact on photocatalytic activity, followed by oxidant concentration and photocatalyst amount. This effect can be explained by longer irradiation times providing greater exposure of the TNTs/zeolite photocatalyst surface to sunlight, producing more hydroxyl radicals that enhance pollutant degradation. Figure 4(b) illustrates the effect of pH and catalyst loading on pH photo-neutralization while keeping irradiation time constant at 180 minutes. The results show that pH values from 3 to 6.5 and catalyst loadings from 1 × 1 cm² to 2 × 1 cm² improved pH neutralization. However, excessive catalyst loading can limit light penetration to the photocatalyst surface, reducing photocatalytic activity. Compared to catalyst loading, pH appears to be the more influential factor in pH neutralization. Figure 4(c) shows the interaction between irradiation time and catalyst loading at a fixed pH of 6.5. The results indicate that, at an irradiation time of 180 minutes, increasing catalyst loading up to approximately 2 × 1 cm² enhances pH photo-neutralization, demonstrating the combined effect of adequate catalyst surface area and sufficient irradiation time.

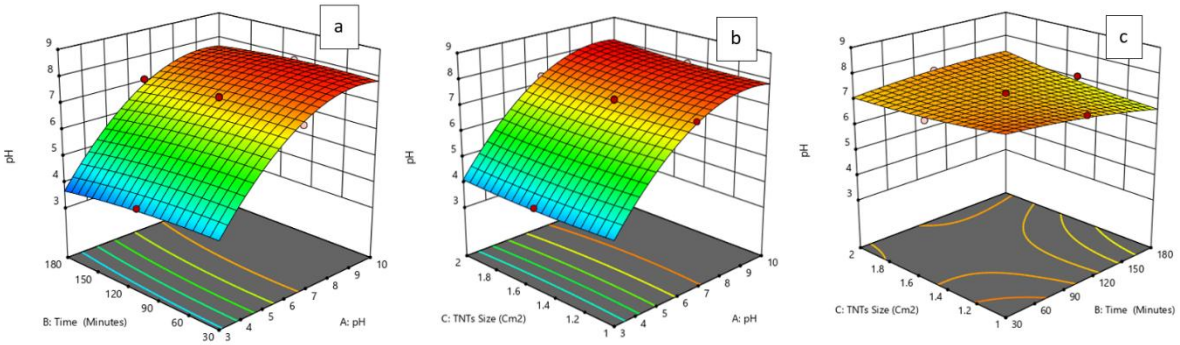

Figure 4. 3-D response surface of pH neutralization using photocatalytic degradation, a) time and pH, b) catalyst and pH, c) catalyst and time.

3.4. Mechanistic interpretation of photocatalytic degradation.

At low pH (pH 3), the surface of TiO_2 is positively charged (below its point of zero charge of ~6.2), which enhances electrostatic attraction with negatively charged organic species, resulting in rapid oxidation and reduction of COD. However, such strong acidity can hinder the assessment of microbial-related biodegradable fractions, so BOD removal was found to be better optimized near pH 6–6.5. Extreme acidity is also impractical from an operational standpoint. Therefore, the optimum conditions for maximum removal were set at a practically feasible, near-neutral pH, even though higher COD removal was observed at lower pH. Incomplete oxidation during photocatalysis may produce intermediate compounds, such as aldehydes or low-molecular-weight acids, before complete mineralization occurs. Nevertheless, COD progressively decreased while DO increased, indicating substantial mineralization rather than partial oxidation. Tsoumachidou et al. [4] reported ~50% COD removal under artificial UV, whereas the present study achieved >60% COD removal under natural sunlight, highlighting the enhanced efficiency of the TNTs/zeolite composite. Maximum removal occurred at pH 3, but such acidic adjustment would require chemical dosing, increasing operational complexity and cost. Therefore, the optimized condition near pH 6.25 is more feasible for actual greywater systems as it does not require intensive pH modification. Under optimal conditions, the treatment complied with Malaysian discharge standards for COD and BOD.

4. Limitations and Future Work

However, there are also some limitations to this study. First and most important is that the process depends on natural sunlight-in different climatic conditions, variations of solar irradiance can imply efficiency in treatment as well as reproducibility of results. Even though irradiance was monitored during experiments implementation at a larger scale would be influenced by seasons and weather variability.Secondly only physicochemical parameters have been addressed in this work; microbial assessment has not been carried out.Gray water may contain microbial contaminants therefore an evaluation on pathogen removal should be done before any intended reuse. Lastly all experiments were performed at laboratory scale hence issues related with reactor design when optimizing hydraulic flow plus penetration light efficiency need further investigation besides long term catalyst reusability together with structural stability TNTs/zeolite which were assumed attainable for sustainable cost effective application. Future research should therefore focus on pilot-scale validation under real operational conditions to evaluate system robustness and treatment consistency. Long-term catalyst stability and regeneration studies are necessary to determine durability and economic feasibility. Further investigation into integrating photocatalysis with biological treatment processes may enhance overall removal efficiency, particularly for biodegradable fractions and microbial contaminants. Finally, comprehensive cost benefit and life-cycle analyses should be conducted to assess economic viability and environmental sustainability for decentralized greywater reuse systems.

5. Conclusions

This study successfully optimized TNTs/zeolite solar photocatalytic treatment of bathroom greywater using RSM. The validated model demonstrated strong predictive accuracy. The system showed promising potential for sustainable greywater reuse. RSM was able to estimate the optimum combination of operational parameters to achieve the highest percentage removal

for greywater treatment. Upper and lower limits of the operating range were used as constraints to determine optimal values. From the experimental results, two experimental runs (Exp. no. 2 and 8, Table 2) showed the highest percentage removal, with all responses above 50% reduction. For Exp. no. 2, with pH 3, 180 minutes of irradiation, and 1 × 1 cm catalyst loading, the removals were 97.74% BOD, 57.62% COD, 83.7% turbidity, 79.66% TSS, with DO increasing to 10.12 mg/L, although the final pH remained acidic at 3.28. Meanwhile, Exp. no. 8 achieved slightly higher COD reduction (68.27%) but slightly lower removal of TSS, BOD, and turbidity (78.06%, 94.22%, and 82.48%, respectively). To obtain the optimized photocatalytic degradation condition for ABGW, lower and upper limits were adjusted to maximize responses. The operational parameters were set within the studied range, aiming for maximum removal. At the RSM-predicted optimum, BOD, COD, TSS, and turbidity were all reduced by over 50%, while pH and DO met greywater quality standards, corresponding to pH 6.245, 180 minutes of irradiation time, and 1 × 1 cm catalyst loading.

Acknowledgement

We gratefully acknowledge the support from the Ministry of Education Malaysia through FRGS Vot K090 and Universiti Tun Hussein Onn Malaysia under the GPPS Grant Vot U777. We also extend our sincere appreciation to Curtin University Malaysia for its facilities and continuous support, which greatly contributed to the success of this research.

References

[1] Mohamed, R. M. S. R.; Al-Gheethi, A. A.; Wurochekke, A. A.; Maizatul, A. Y.; Matias-Peralta, H. M.; Mohd Kassim, A. H. (2018). Nutrients removal from artificial bathroom greywater using Botryococcus sp. Strain. *IOP Conference Series: Earth and Environmental Science*, *140*(1). https://doi.org/10.1088/1755-1315/140/1/012026.

[2] Borges, M. E.; Sierra, M.; Cuevas, E.; García, R. D.; Esparza, P. (2016). Photocatalysis with solar energy: Sunlight-responsive photocatalyst based on TiO2 loaded on a natural material for wastewater treatment. *Solar Energy*, *135*, 527–535. https://doi.org/10.1016/j.solener.2016.06.022.

[3] Donner, E.; Eriksson, E.; Revitt, D. M.; Scholes, L.; Lützhøft, H. C. H.; Ledin, A. (2010). Presence and fate of priority substances in domestic greywater treatment and reuse systems. *Science of the Total Environment*, *408*(12), 2444–2451. https://doi.org/10.1016/j.scitotenv.2010.02.033.

[4] Tsoumachidou, S.; Velegraki, T.; Antoniadis, A.; Poulios, I. (2016). Greywater as a sustainable water source: A photocatalytic treatment technology under artificial and solar illumination. *Journal of Environmental Management*, 1–10. https://doi.org/10.1016/j.jenvman.2016.08.025.

[5] Dai, G.; Huang, J.; Chen, W.; Wang, B.; Yu, G.; Deng, S. (2014). Major pharmaceuticals and personal care products (PPCPs) in wastewater treatment plant and receiving water in Beijing, China, and associated ecological risks. *Bulletin of Environmental Contamination and Toxicology*, *92*(6), 655–661. https://doi.org/10.1007/s00128-014-1247-0.

[6] Eriksson, E.; Auffarth, K.; Henze, M.; Ledin, A. (2002). Characteristics of grey wastewater. 4, 85–104.

[7] Yang, X.; Chen, F.; Meng, F.; Xie, Y.; Chen, H.; Young, K.; … Fu, W. (2013). Occurrence and fate of PPCPs and correlations with water quality parameters in urban riverine waters of the Pearl River Delta, South China. *Environmental Science and Pollution Research*, *20*(8), 5864–5875. https://doi.org/10.1007/s11356-013-1641-x.

[8] Malato, S.; Fernández-Ibáñez, P.; Maldonado, M. I.; Blanco, J.; Gernjak, W. (2009). Decontamination and disinfection of water by solar photocatalysis: Recent overview and trends.

Catalysis Today, *147*(1), 1–59. https://doi.org/10.1016/j.cattod.2009.06.018.

[9] Robinson, J.; Davidson, P.; Bhattarai, R. (2014). The efficiency of a Pyramid-shaped solar still. 1(1).

[10] Gao, X.; Zhang, X.; Wang, Y.; Peng, S.; Yue, B.; Fan, C. (2015). Photocatalytic degradation of carbamazepine using hierarchical BiOCl microspheres: Some key operating parameters, degradation intermediates and reaction pathway. *Chemical Engineering Journal*, *273*, 156–165. https://doi.org/10.1016/j.cej.2015.03.063.

[11] Ismail, L.; Rifai, A.; Ferronato, C.; Fine, L.; Jaber, F.; Chovelon, J. M. (2016). Towards a better understanding of the reactive species involved in the photocatalytic degradation of sulfaclozine. *Applied Catalysis B: Environmental*, *185*, 88–99. https://doi.org/10.1016/j.apcatb.2015.12.008.

[12] Ji, Y.; Zhou, L.; Ferronato, C.; Yang, X.; Salvador, A.; Zeng, C.; Chovelon, J. M. (2013). Photocatalytic degradation of atenolol in aqueous titanium dioxide suspensions: Kinetics, intermediates and degradation pathways. *Journal of Photochemistry and Photobiology A: Chemistry*, *254*, 35–44. https://doi.org/10.1016/j.jphotochem.2013.01.003.

[13] Zhang, Q.; Zhu, J.; Wang, Y.; Feng, J.; Yan, W.; Xu, H. (2014). Electrochemical assisted photocatalytic degradation of salicylic acid with highly ordered TiO2 nanotube electrodes. *Applied Surface Science*, *308*, 161–169. https://doi.org/10.1016/j.apsusc.2014.04.125.

[14] Hoque, M. A.; Guzman, M. I. (2018). Photocatalytic activity: Experimental features to report in heterogeneous photocatalysis. *Materials*, *11*(10), 1990.

[15] Godheja, J.; SK, S.; Siddiqui, S. A.; DR, M. (2016). Xenobiotic Compounds Present in Soil and Water: A Review on Remediation Strategies. *Journal of Environmental & Analytical Toxicology*, *6*(5). https://doi.org/10.4172/2161-0525.1000392.

[16] Jallouli, N.; Elghniji, K.; Trabelsi, H.; Ksibi, M. (2017). Photocatalytic degradation of paracetamol on TiO2 nanoparticles and TiO2/cellulosic fiber under UV and sunlight irradiation. *Arabian Journal of Chemistry*, *10*, S3640–S3645. https://doi.org/10.1016/j.arabjc.2014.03.014.

[17] Mano, T.; Nishimoto, S.; Kameshima, Y.; Miyake, M. (2015). Water treatment efficacy of various metal oxide semiconductors for photocatalytic ozonation under UV and visible light irradiation. *Chemical Engineering Journal*, *264*, 221–229. https://doi.org/10.1016/j.cej.2014.11.088.

[18] Thomas, M.; Naikoo, G. A.; Sheikh, M. U. D.; Bano, M.; Khan, F. (2016). Effective photocatalytic degradation of Congo red dye using alginate/carboxymethyl cellulose/TiO2 nanocomposite hydrogel under direct sunlight irradiation. *Journal of Photochemistry and Photobiology A: Chemistry*, *327*, 33–43. https://doi.org/10.1016/j.jphotochem.2016.05.005.

[19] Ding, S. L.; Wang, X. K.; Jiang, W. Q.; Meng, X.; Zhao, R. S.; Wang, C.; Wang, X. (2013). Photodegradation of the antimicrobial triclocarban in aqueous systems under ultraviolet radiation. *Environmental Science and Pollution Research*, *20*(5), 3195–3201. https://doi.org/10.1007/s11356-012-1239-8.

[20] Giri, R. R.; Ozaki, H.; Ota, S.; Takanami, R.; Taniguchi, S. (2010). Degradation of common pharmaceuticals and personal care products in mixed solutions by advanced oxidation techniques. *International Journal of Environmental Science and Technology*, *7*(2), 251–260. https://doi.org/10.1007/BF03326135.

[21] Kaneco, S.; Rahman, M. A.; Suzuki, T.; Katsumata, H.; Ohta, K. (2004). Optimization of solar photocatalytic degradation conditions of bisphenol A in water using titanium dioxide. *Journal of Photochemistry and Photobiology A: Chemistry*, *163*(3), 419–424. https://doi.org/10.1016/j.jphotochem.2004.01.012.

[22] Zhou, F.; Yan, C.; Liang, T.; Sun, Q.; Wang, H. (2018). Photocatalytic degradation of Orange G using sepiolite-TiO2 nanocomposites: Optimization of physicochemical parameters and kinetics studies. *Chemical Engineering Science*, *183*, 231–239. https://doi.org/10.1016/j.ces.2018.03.016.

[23] Wurochekke, A. A.; Mohamed, R. M. S.; Al-Gheethi, A. A.; Atiku, H.; Amir, H. M.; Matias-

Peralta, H. M. (2016). Household greywater treatment methods using natural materials and their hybrid system. *Journal of Water and Health*, *14*(6), 914–928.

[24] Oteng-Peprah, M.; Acheampong, M. A.; DeVries, N. K. (2018). Greywater characteristics, treatment systems, reuse strategies and user perception—a review. *Water, Air, & Soil Pollution*, *229*(8), 255.

[25] Hourlier, F.; Masse, A.; Jaouen, P.; Lakel, A.; Gerente, C.; Faur, C.; Cloirec, P. Le. (2010). Formulation of synthetic greywater as an evaluation tool for wastewater recycling technologies. *Environmental*, *31*(2), 37–41. https://doi.org/10.1080/09593330903431547.

[26] Nischk, M.; Mazierski, P.; Wei, Z.; Siuzdak, K. (2016). Enhanced photocatalytic, electrochemical and photoelectrochemical properties of TiO2 nanotubes arrays modified with Cu, AgCu and Bi nanoparticles obtained via radiolytic reduction. *Applied Surface Science*, *387*, 89–102. https://doi.org/10.1016/j.apsusc.2016.06.066.

[27] Lai, C. W.; Sreekantan, S. (2011). Effect of applied potential on the formation of self-organized TiO2 nanotube arrays and its photoelectrochemical response. *Journal of Nanomaterials*, 2011(iii). https://doi.org/10.1155/2011/142463.

[28] Wang, C.; Li, Y.; Shi, H.; Huang, J. (2015). Preparation and characterization of natural zeolite supported nano TiO2 photocatalysts by a modified electrostatic self-assembly method. *Surface and Interface Analysis*, *47*(1), 142–147. https://doi.org/10.1002/sia.5686.

[29] Mohamed, R. M. S. R.; Chan, C. M.; Senin, H.; Kassim, A. H. M. (2014). Feasibility of the direct filtration over peat filter media for bathroom greywater treatment. *Journal of Materials and Environmental Science*, *5*(6), 2021–2029.

[30] Rastegar, M.; Shadbad, K. R.; Khataee, A. R.; Pourrajab, R. (2012). Optimization of photocatalytic degradation of sulphonated diazo dye C.I. Reactive Green 19 using ceramic-coated TiO2 nanoparticles. *Environmental Technology*, *33*(9), 995–1003. https://doi.org/10.1080/09593330.2011.604859.

[31] Chaibakhsh, N.; Ahmadi, N.; Zanjanchi, M. A. (2016). Optimization of photocatalytic degradation of neutral red dye using TiO2 nanocatalyst via Box-Behnken design. *Desalination and Water Treatment*, *57*(20), 9296–9306. https://doi.org/10.1080/19443994.2015.1030705.

[32] Barakat, M. A. (2011). Adsorption and photodegradation of Procion yellow H-EXL dye in textile wastewater over TiO2 suspension. *Journal of Hydro-Environment Research*, *5*(2), 137–142. https://doi.org/10.1016/j.jher.2010.03.002.

[33] Montazerozohori, M.; Nasr-Esfahani, M.; Joohari, S. (2012). Photocatalytic degradation of an organic dye in some aqueous buffer solutions using nano titanium dioxide: A kinetic study. *Environment Protection Engineering*, *38*(3), 45–55. https://doi.org/10.5277/EPE120305.

[34] Giwa, A.; Nkeonye, P. O.; Bello, K. A.; Kolawole, K. A. (2012). Photocatalytic decolourization and degradation of C.I. Basic Blue 41 using TiO2 nanoparticles. *Journal of Environmental Protection*, *3*(9), 1063–1069. https://doi.org/10.4236/jep.2012.39124.

[35] Pare, B.; Swami, D.; More, P.; Qureshi, T.; Thapak, T. R. (2011). Mineralization of methylene violet dye using titanium dioxide in presence of visible light. *International Journal of Chemical Sciences*, *9*(4), 1685–1697.

[36] Ghaly, M. Y.; Farah, J. Y.; Fathy, A. M. (2007). Enhancement of decolorization rate and COD removal from dyes containing wastewater by the addition of hydrogen peroxide under solar photocatalytic oxidation. *Desalination*, *217*(1–3), 74–84. https://doi.org/10.1016/j.desal.2007.01.013.

[37] Mahmoodi, N. M.; Arami, M.; Limaee, N. Y.; Tabrizi, N. S. (2005). Decolorization and aromatic ring degradation kinetics of Direct Red 80 by UV oxidation in the presence of hydrogen peroxide utilizing TiO2 as a photocatalyst. *Chemical Engineering Journal*, *112*(1–3), 191–196. https://doi.org/10.1016/j.cej.2005.07.008.

[38] Dostanić, J.; Lončarević, D.; Rožić, L.; Petrović, S.; Mijin, D.; Jovanović, D. M. (2013). Photocatalytic degradation of azo pyridone dye: Optimization using response surface methodology. *Desalination and Water Treatment*, *51*(13–15), 2802–2812. https://doi.org/10.1080/19443994.2012.750699.